Journal of Applied Mechanics and Technical Physics, Vol. 36, No. 4, 1995

INFLUENCE OF A CRACK IN A FLOATING ELASTIC PLATE ON THE PROPAGATION OF FLEXURAL GRAVITATIONAL WAVES

A. E. Bukatov and D. D. Zav'yalov

UDC 532.596

An analysis of the influence of a crack in a floating elastic plate on the propagation of flexural gravitational surface waves in a basin of finite depth has been performed. The dependences of the distribution of reflection and transmission amplitude coefficients over the oscillation period on the plate characteristics, on the longitudinal compressive force, and on the basin depth have been studied, taking into account the contribution of near-edge modes to the formation of wave perturbations. The surging of waves toward the edge of an ice plate has been considered in [1–3]. Contact conditions at the crack and their applications to the solution of the problem of the wave reflection in deep water are the subjects of [4].

1. Assume that two half-infinite elastic plates, modeling, in particular, an ice cover with a crack, float on the surface of a basin with a constant finite depth H. We consider the influence of the crack on flexural gravitational surface waves propagating normally to the crack. The liquid motion is assumed to be potential. The origin of coordinates with the z axis pointed upward is placed at the basin bottom. The regions of water covered by plates with thicknesses h_1 and h_2 are situated to the left ($x < 0$) and to the right ($x > 0$) of the vertical axis, respectively. The potentials of liquid motion velocity in these regions are denoted by $\Phi_1(x,z,t) = \varphi_1(x,z)e^{i\omega t}$ and $\Phi_2(x,z,t) = \varphi_2(x,z)e^{i\omega t}$ (ω is the given frequency of the wave incident from the region $x < 0$).

We consider the dependences of the distributions of disturbance reflection and transmission amplitude coefficients over the incident wave period on the basin depth, plate characteristics, and compressive force. In the chosen frame, this problem reduces to solving the Laplace equations

$$\Delta\varphi_j = 0 \tag{1.1}$$

with boundary conditions at the basin surface ($z = H$)

$$d_j\frac{\partial^5\varphi_j}{\partial z\partial x^4} - q_j\frac{\partial^3\varphi_j}{\partial z\partial x^2} + (1 - æ_j\omega^2)\frac{\partial\varphi_j}{\partial z} - \frac{\omega^2}{g}\varphi_j = 0 \tag{1.2}$$

and at the bottom ($z = 0$)

$$\frac{\partial\varphi_j}{\partial z} = 0, \tag{1.3}$$

where

$$d_j = \frac{E_j h_j^3}{12\rho g(1-\nu_j^2)}; \qquad æ_j = \frac{\rho_j h_j}{\rho g}; \qquad q_j = \frac{q_{1j}}{\rho g}; \qquad j = \begin{cases} 1, & -\infty < x < 0, \\ 2, & 0 < x < +\infty; \end{cases}$$

E_j, h_j, ρ_j, ν_j are the normal elasticity coefficient, thickness, density, and Poisson's ratio of the plate; q_{1j} is the compressive force; ρ is the water density. In addition, the potentials and velocities of horizontal wave flows should satisfy the continuity conditions at the contact boundary

$$\varphi_1 = \varphi_2, \quad \frac{\partial\varphi_1}{\partial x} = \frac{\partial\varphi_2}{\partial x}, \quad 0 < z < H, \quad x = 0, \tag{1.4}$$

Marine Hydrophysics Institute, Sevastopol' 335000, Ukraine. Translated from Prikladnaya Mekhanika i Tekhnicheskaya Fizika, Vol. 36, No. 4, pp. 170–175, July–August, 1995. Original article submitted August 12, 1994.

 0021-8944/95/3604-0628 $12.50

and the free-edge conditions which are the equality to zero of the flexural moment and shearing force at the plate's edges [4]:

$$\frac{\partial^3\varphi_j}{\partial z\partial x^2} = \frac{\partial^4\varphi_j}{\partial z\partial x^3} = 0. \tag{1.5}$$

Applying the variable separation method to Eqs. (1.1)–(1.3), we get the dispersion relations

$$\omega^2 = \frac{(d_j r_j^4 - q_j r_j^2 + 1)\, r_j\, g \tanh(r_j H)}{1 + æ_j\, r_j\, g \tanh(r_j H)}, \tag{1.6}$$

which connect the phase characteristics of wave disturbances in the regions $x < 0$ and $x > 0$, respectively. Equation (1.6) has four real roots $\pm r_j$, four pairs of complex conjugate roots $\beta_j \pm i\alpha_j$ and $-\beta_j \pm i\alpha_j$, and countable sets of pure imaginary roots $\pm ir_{jn}$ $(n = 1, 2, 3, \ldots)$. Taking into account the boundedness of the potentials φ_1 at $x \to \infty$, φ_2 at $x \to -\infty$, and the absence of an undamped wave surging toward the crack from the region $x > 0$, we write

$$\varphi_1 = Ie^{-ir_1 x}\cosh(r_1 z) + R_* e^{ir_1 x}\cosh(r_1 z) + R_1 e^{+(\alpha_1 + i\beta_1)x}\cos[(\alpha_1 + i\beta_1)z]$$

$$+R_2 e^{+(\alpha_1 - i\beta_1)x}\cos[(\alpha_1 - i\beta_1)z] + \sum_{n=1}^{\infty} A_n e^{r_{1n}x}\cos(r_{1n}z); \tag{1.7}$$

$$\varphi_2 = T_* e^{-ir_2 x}\cosh(r_2 z) + T_1 e^{-(\alpha_2 + i\beta_2)x}\cos[(\alpha_2 + i\beta_2)z]$$

$$+T_2 e^{-(\alpha_2 - i\beta_2)x}\cos[(\alpha_2 - i\beta_2)z] + \sum_{n=1}^{\infty} B_n e^{-r_{2n}x}\cos(r_{2n}z). \tag{1.8}$$

All the amplitude coefficients of the potentials φ_1, φ_2 are complex. I, R_*, T_* represent incident, reflected, and transmitted undamped progressive waves characterized by the roots $-r_1$, r_1, and $-r_2$ of related dispersion equations. The coefficients $R_{1,2}$ and $T_{1,2}$ correspond to damped progressive waves due to the flexural stiffness of the plate. They are determined by the roots $\pm\beta_1 - i\alpha_1$ and $\pm\beta_2 + i\alpha_2$ of Eqs. (1.6). The near-edge modes [2, 3], which exist on each side of the crack and decrease exponentially away from the crack are represented by the roots r_{jn} of Eqs. (1.6) and by the coefficients A_n, B_n in the regions $x < 0$ and $x > 0$, respectively.

2. We shall consider the matching problem for potentials and their derivatives as variational. Therefore, finding the velocity potentials reduces to minimization of the error functional for matching with conditions (1.4), (1.5). To pass on to a search for the absolute extremum, we write the error functional [3] as

$$\varepsilon = \delta\int_0^H |\varphi_1 - \varphi_2|^2 dz + \mu\int_0^H \left|\frac{\partial\varphi_1}{\partial x} - \frac{\partial\varphi_2}{\partial x}\right|^2 dz + \gamma\sum_{j=1}^{2}\left\{\left(\frac{\partial^3\varphi_j}{\partial z\partial x^2}\right)^2 + \left(\frac{\partial^4\varphi_j}{\partial z\partial x^3}\right)^2\right\}, \tag{2.1}$$

where δ, μ, and γ are unknown Lagrange multipliers. After substituting (1.7), (1.8) into (2.1) and evaluating the integrals, the error functional takes the matrix form

$$\varepsilon = \mathbf{c}^{\mathrm{t}}(\delta\mathbf{Q}_p + \mu\mathbf{Q}_d + \gamma\mathbf{Q}_e)\,\mathbf{c}. \tag{2.2}$$

Here $\mathbf{c}$ is the column-vector of the real and imaginary parts of unknown coefficients; the matrices $\mathbf{Q}_p$, $\mathbf{Q}_d$, and $\mathbf{Q}_e$ characterize the matching discrepancies of potentials, of their derivatives, and those of fulfillment of the free-edge condition at the edges on each side of the crack, respectively; the index t means transposition.

We put the amplitude of the incident wave potential to be equal to unity, thus excluding a trivial solution of the problem. This conjecture is equivalent to solving the matrix equation

$$\mathbf{c}^{\mathrm{t}}\mathbf{K}\mathbf{c} - 2\mathbf{v}^{\mathrm{t}}\mathbf{c} + \mathbf{v}^{\mathrm{t}}\mathbf{v} = 0, \tag{2.3}$$

where the elements of the vector $\mathbf{v}$ are arranged so that unity corresponds to the amplitude I and zeros to

the other coefficients; $\mathbf{K}$ is the square matrix defined via

$$\mathbf{Kc} = \mathbf{v}. \tag{2.4}$$

Equation (2.3) is an additional condition to (2.2), and hence we write finally the error functional as

$$\mathbf{c}^{\mathrm{t}}(\delta\mathbf{Q}_p + \mu\mathbf{Q}_d + \gamma\mathbf{Q}_e + \eta\mathbf{K})\mathbf{c} - 2\eta\mathbf{v}^{\mathrm{t}}\mathbf{c} \tag{2.5}$$

(η is the additional Lagrange multiplier). Minimization of functional (2.5) is equivalent [5] to solving the matrix equation

$$(\delta\mathbf{Q}_p + \mu\mathbf{Q}_d + \gamma\mathbf{Q}_e + \eta\mathbf{K})\mathbf{c} = \eta\mathbf{v}. \tag{2.6}$$

Since $\mathbf{Q} = (\delta\mathbf{Q}_p + \mu\mathbf{Q}_d + \gamma\mathbf{Q}_e + \eta\mathbf{K})$ is the ill-conditioned sparse matrix, direct methods for solving linear equation systems, as applied to (2.6), may lead to excessive computational efforts [6] and are inadequate in this case. It is more reasonable to use iterative methods, e.g., the adjoint gradient method. An iterative process may be represented in the form [7]

$$\mathbf{c}^{(i+1)} = \mathbf{G}\mathbf{c}^{(i)} + \mathbf{F}, \quad i = 0, 1, 2, 3, \ldots .$$

Here, the real transition matrix $\mathbf{G}$ for the nonsingular split matrix $\mathbf{S}$ has the structure $\mathbf{G} = \mathbf{E} - \mathbf{S}^{-1}\mathbf{Q}$ ($\mathbf{E}$ is the unit matrix and $\mathbf{F} = \mathbf{S}^{-1}\eta\mathbf{v}$). Although $\mathbf{Q}$ is a symmetric positive-definite matrix and the adjoint gradient method in exact arithmetic should converge to a true solution of Eq. (2.4) in a finite number of iterations, round-off errors violate this property. The following inequality [6] allows us to estimate the convergency speed:

$$\|\mathbf{c}^{(i)} - \mathbf{c}\|_2 \leqslant 2\sqrt{\sigma}\, M^{(i)} \|\mathbf{c}^{(0)} - \mathbf{c}\|_2,$$

where $\sigma = \|\mathbf{Q}\|_2 \cdot \|\mathbf{Q}^{-1}\|_2$ is the spectral condition number of the matrix $\mathbf{Q}$; $M = (\sqrt{\sigma} - 1)/(\sqrt{\sigma} + 1)$. We note that the greater σ (the worse the conditionality of $\mathbf{Q}$), the stronger the convergency speed slows down. Therefore, the adjoint gradient method is always used with a certain kind of preconditioning. The procedure is reduced to the construction of the new linear system

$$\mathbf{W}(\mathbf{E} - \mathbf{G})\mathbf{c} = \mathbf{WF} \tag{2.7}$$

($\mathbf{W}$ is the symmetrization matrix), which has the same solution as the original one (2.6), and the coefficient matrix $\mathbf{W}$ of the new system is symmetric and positive-definite and possesses, generally, a lesser spectral condition number compared with the coefficient matrix $\mathbf{Q}$ of the original system. However, minimization of the value σ is not the only aim of the preconditioning. It is necessary to use a wider property spectrum of the matrix $\mathbf{W}(\mathbf{E} - \mathbf{G})\mathbf{W}^{-1}$ [6]. Furthermore, if the conditionality of the coefficient matrix of the preconditioned system is $\sigma = 1$, then the preconditioned linear equation system (2.7) is equivalent to the original one (2.6).

A diagonal matrix with elements $\mathbf{Q}_p(k, k)$, $k = 1, 2, \ldots, n$, has been chosen as the symmetrization matrix $\mathbf{W}$, and $\mathbf{S} = \mathbf{W}^*\mathbf{W}$ is the split matrix. The Lagrange multipliers δ, μ, γ, η for the convergence optimization were chosen as in [3]. The number n of near-edge damped modes summed in numerical computations was taken so as to satisfy the required accuracy from the balance of energy flux densities through a closed surface bounding a given liquid volume. The volume is limited by part of the basin surface, a region of the impenetrable bottom, and vertical walls equidistant from the crack. The energy flux density J in the uniformly compressed elastic plate at its flexural oscillations with amplitude ξ was taken into account [4] according to the formula

$$J = \rho g \left[d_j \left(\frac{\partial^3 \xi}{\partial x^3} \frac{\partial \xi}{\partial t} - \frac{\partial^2 \xi}{\partial x^2} \frac{\partial^2 \xi}{\partial x \partial t} \right) - q_j \frac{\partial \xi}{\partial x} \frac{\partial \xi}{\partial t} \right].$$

3. Quantitative estimation of the dependence of distributions of the reflection R and transmission T amplitude coefficients related to the incident wave amplitude over the oscillation period τ on the plate characteristics and on the basin depth was carried out for an ice plate with $\rho = 1025$ kg/m^3, $\rho_{1,2} = 870$ kg/m^3, $\nu_{1,2} = 0.3$, $h_1 \leqslant h_2$. The ice thickness was $h_j = 0$–2 m, its elasticity coefficient $E_j = 3 \cdot 10^7$–$3 \cdot 10^9$ N/m^2, the quantity $q_j = 0$–$1.3\sqrt{d_j}$ m^2 (characterizing the ice compression degree), and the basing depth $H = 10$–50 m. Waves with periods τ up to 20 sec were considered.

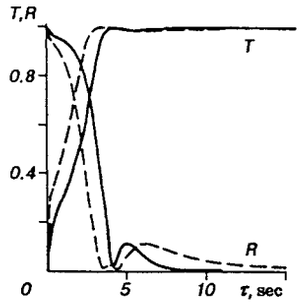

Fig. 1

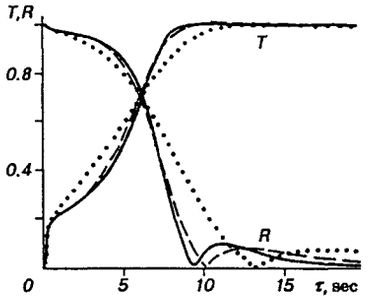

Fig. 2

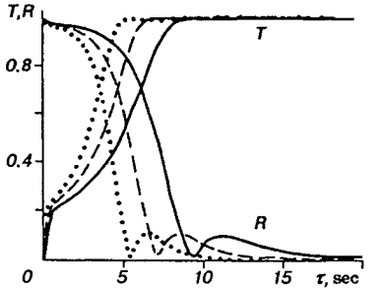

Fig. 3

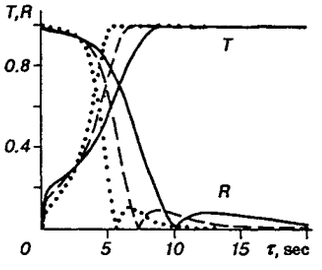

Fig. 4

The quantities R and T were specified through velocity potentials (1.7), (1.8) from the continuity condition for oscillations on the basin surface which implies that the vertical component of the liquid velocity is equal to that of the ice plate on each side of the crack. Some of the results that clearly show the possible manifestations of distinctive features of the wave regime are presented at Figs. 1–6. Analysis of the calculation results shows that neglecting the damped near-edge modes, which rules out the possibility of matching the potentials φ_1, φ_2 and the horizontal velocity components $\partial\varphi_1/\partial x$ and $\partial\varphi_2/\partial x$ throughout the liquid depth under the crack ($x = 0$), does not reflect to the full extent the physical essence of the studied phenomenon. This can be seen most clearly for small ($\tau < 5$ sec) and intermediate (5 sec $< \tau <$15 sec) periods.

For small periods there exists a significant underestimation of R and overestimation of T which may reach an order of 50%. This is evident from a comparison of plots in Fig. 1 for $H = 25$ m, $h_1 = h_2 = 1$ m, $q_1 = q_2 = 0$, and $E = 3 \cdot 10^9$ N/m^3 (solid lines correspond to matching throughout the depth, while dashed lines are for matching at the basin surface). For intermediate periods, differences in the matching conditions for potentials and horizontal velocities at $x = 0$, scarcely affecting the coefficient T, may lead to either a decreased (for shallow water) or increased (for deep water) value of R.

The dependences of R and T distributions over the oscillation period on the basin depth, ice thickness, its stiffness, and ice compression degree are plotted for $h = 2$ m (Figs. 2, 4), $q = 0$ (Figs. 2–4), $H = 50$ m (Fig. 3), $H = 25$ m (Fig. 4, 5), $h = 1$ m (Fig. 5). They are obtained for the same ice conditions on each side of the crack with elasticity coefficient $E = 3 \cdot 10^9$ N/m^3 (except Fig. 4). Dotted, dashed, and solid lines correspond to depths of 10, 25, 50 m (Fig. 2); ice thicknesses of 0.5, 1, 2 m (Fig. 3); $E = 3 \cdot 10^7$, $3 \cdot 10^8$, $3 \cdot 10^9$ N/m^3 (Fig. 4); and $q_j = 0$, $\sqrt{d_j}$, $1.3\sqrt{d_j}$ (Fig. 5).

Calculation results show that at a fixed ice thickness a period τ_* exists such that $R = T = 1/\sqrt{2}$. It is essentially independent of the basin depth and is determined only by the plate parameters. The value τ_* grows with an increase in the ice elasticity and thickness, as can be seen from a comparison of the plots in Figs. 2–4. In addition, under certain conditions there may exist a period τ_0 of the full transmission of waves

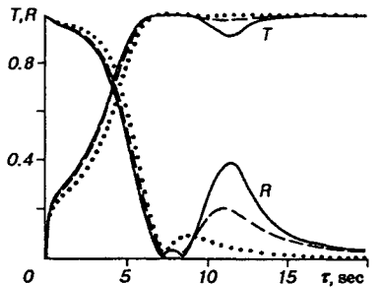

Fig. 5

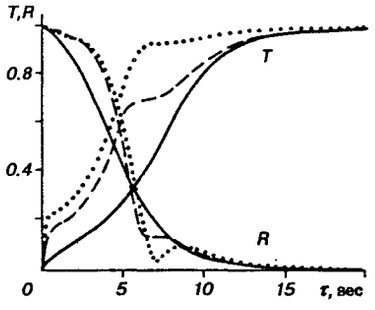

Fig. 6

with an intermediate wavelength through the crack in the ice cover; the value τ_0 shifts to smaller periods with the increased basin depth. At $\tau_0 < \tau < \infty$, the function $T(\tau)$ has a minimum whose value is close to unity. The period of the full transmission diminishes with decreased cylindrical ice stiffness.

The amplitude transmission T (reflection R) coefficient decreases (increases) at periods $\tau < \tau_*$, and increases (decreases) at $\tau > \tau_*$ as the depth H increases. Increased ice thickness leads to decreased T and increased R. An increase in the ice compression degree in the interval considered makes the transmission (reflection) coefficient stronger (weaker) at $\tau < \tau_0$. If $\tau > \tau_0$, the directionality of the influence of compression on R and T is changed, being pronounced within a finite interval of periods (Fig. 5). Also, under compression the full reflection may take place at two different periods.

With the ice thickness decreased in a region from which a progressive wave surges toward the crack, the perturbation picture approaches the picture formed in the case of a wave surging toward the crack from open water [3]. The plots in Fig. 6 at $h_2 = 1$ m, $q_1 = q_2 = 0$, $E = 3 \cdot 10^9$ N/m^3 and $H = 25$ m illustrate the dependence of the transmission and reflection coefficients on variations of h_1 (solid, dashed, and dotted lines correspond to $h_1 = 0.1$, 0.6, and 0.9 m).

REFERENCES

1. M. Weitz and J. B. Keller, "Reflection of water waves from floating ice in water of finite depth," *Commun. Pure Appl. Math.*, **3**, 305–318 (1950).
2. D. E. Kheisin, *Dynamics of the Ice Cover* [in Russian], Gidrometeoizdat, Leningrad (1967).
3. C. Fox and V. A. Squire, "Reflection and transmission characteristics at the edge of shore fast sea ice," *J. Geophys. Res.*, **95**, No. 7, 11629–11639 (1990).
4. V. N. Krasil'nikov, "On the solution of some boundary contact problems of linear hydrodynamics," *Prikl. Mat. Mekh.*, **25**, No. 4, 764–768 (1967).
5. Ya. B. Zel'dovich and A. D. Myshkis, *Elements of Applied Mathematics* [in Russian], Nauka, Moscow, (1967).
6. J. M. Ortega, *Introduction to Parallel and Vector Solution of Linear Systems* [Russian translation], Mir, Moscow (1991).
7. L. Hageman and D. M. Young, *Applied Iterative Methods* [Russian translation], Mir, Moscow (1991).